Role of the edge orbits in the semiclassical quantization of the stadium billiard

1994 J. Phys. A: Math. Gen. 27 1599

(http://iopscience.iop.org/0305-4470/27/5/023)

J. Phys. A: Math. Gen. 27 (1994) 1599–1607. Printed in the UK

Role of the edge orbits in the semiclassical quantization of the stadium billiard

D Alonso and P Gaspard

Faculté des Sciences and Centre for Nonlinear Phenomena and Complex Systems, Université Libre de Bruxelles, Campus Plaine, Code Postal 231, Blvd du Triomphe, B-1050 Brussels, Belgium

Received 12 July 1993

Abstract. In the periodic orbit quantization of the stadium billiard, we show that important contributions may be due to the edge orbits, i.e. to orbits bouncing between points where the curvature of the boundary is discontinuous. We explicitly show that these edge orbits are necessary to reproduce several amplitudes of the length spectrum defined by the Fourier transform of the staircase function. In this way, we explain some features overlooked in recent experiments on microwave cavities.

1. Introduction

Recently a lot of works have been devoted to the quantization of classically chaotic systems [1–4]. Among the systems which have been used as vehicles for such studies, the stadium billiard is probably the most famous. The great interest in this billiard is due to the proof by Bunimovich that its classical dynamics is chaotic and has the K-property [5]. If most periodic orbits of this billiard are unstable with positive Lyapunov exponents, however, the periodic orbits bouncing between the parallel walls are only marginally unstable with zero Lyapunov exponents. This continuous family of bouncing-ball orbits is of zero Lebesgue measure in phase space so that it does not prevent the classical dynamics from being chaotic.

Nevertheless, a recent microwave experiment [6] has shown that these bouncing-ball orbits may have important consequences on the spectrum of the eigenvalues of the Helmholtz equation

$$(\Delta + k^2)\psi = 0 \tag{1}$$

solved with Dirichlet boundary conditions on the border of the stadium billiard. This experiment has measured the frequencies of the eigenmodes of a quasi two-dimensional superconducting microwave cavity shaped like a quarter of a stadium billiard. The quality of the experimental data has enabled the authors of [6] to reconstruct the staircase function defined as

$$N(k) = \sum_{j=1}^{\infty} \theta(k - k_j) \tag{2}$$

where the wavenumbers k_j of the eigenmodes are proportional to the eigenfrequencies and where $\theta(x)$ denotes the Heaviside function. The results of the experiment have confirmed the theoretical suggestion that the staircase function can be decomposed into [7–9]

$$N_{\text{exact}}(k) \sim N_{\text{av}}(k) + N^{(\alpha)}(k) + N^{(\beta)}(k) \qquad \text{for} \quad k \to \infty . \tag{3}$$

0305-4470/94/051599+09$19.50

$N_{av}(k)$ is the average staircase function given by the Weyl formula plus corrections due to the perimeter and the corners. $N_{av}(k)$ is a monotonic contribution given by a series of powers of k^{-1} starting at $\mathcal{O}(k^2)$. $N^{(\alpha)}(k)$ is an oscillating contribution of order $\sqrt{k}$ due to the marginally unstable periodic orbits and its expression was derived by Berry and Tabor [9]. $N^{(\beta)}(k)$ is the oscillating contribution of order k^0 due to the unstable periodic orbits, which is given by the Gutzwiller trace formula [8]. Because of its order of magnitude, the contribution $N^{(\alpha)}(k)$ of the bouncing-ball orbits dominates the oscillatory part of the staircase function. Moreover, the spectrum of the lengths of the periodic orbits emerging in the semiclassical limit $k \to \infty$ was obtained in [6] from the Fourier transform

$$S(\ell) = \left| \int_{k_{\min}}^{k_{\max}} \mathrm{d}k \, \mathrm{e}^{\mathrm{i}k\ell} \left[N_{\mathrm{exact}}(k) - N_{\mathrm{av}}(k) \right] \right|^2 . \tag{4}$$

However, several features of the experimental length spectrum do not seem to be explained by the preceding decomposition (3). Even after substraction of the Berry–Tabor contribution due to the bouncing-ball orbits, peaks remain in the length spectrum at multiples of the length of the bouncing-ball orbits. These peaks cannot be explained by the unstable periodic orbits of the Gutzwiller contribution since none of them has the length of the bouncing-ball orbits.

We have carried out a numerical calculation of the same quantities for the full stadium billiard rather than for a quarter of it and it turns out that the discrepancy is even more important for the full billiard. The purpose of this paper is to give an explanation of the remaining peaks in terms of the periodic orbits at the edge of the continuous family of bouncing-ball orbits. These edge periodic orbits—here we shall call them periodic orbits of $\alpha\beta$-type—are bouncing at the matching points between the straight walls and the semicircles closing the stadium. We show that these $\alpha\beta$-orbits contribute to the staircase function at the same order k^0 as the Gutzwiller contributions but with a new type of amplitude which differs from the amplitude derived by Gutzwiller and which cannot be obtained by a symmetry argument.

The paper is organized as follows. In section 2, we introduce the main quantities and expressions used in the quantization. In section 3, the different terms entering the semiclassical approximation of $N(k)$ are analysed and the contribution of the shortest $\alpha\beta$-orbit is evaluated. Our numerical results are discussed in section 4 and conclusions are drawn in section 5.

2. General methods

Using the Green theorem and the two-dimensional free Green function $G_0(\boldsymbol{r}, \boldsymbol{r}') = -(\mathrm{i}/4)H_0^{(1)}(k|\boldsymbol{r} - \boldsymbol{r}'|)$, the Helmholtz equation (1) with Dirichlet boundary conditions can be transformed into the integral equation

$$u(s) = 2 \oint \mathrm{d}s' \frac{\partial}{\partial n} G_0\big[\boldsymbol{r}(s), \boldsymbol{r}'(s')\big] u(s') \equiv \big(\hat{Q}u\big)(s) \tag{5}$$

for the gradient of the wavefunction normal to the boundary of the billiard, $u(s) = \partial\psi/\partial n$ [10, 11]. In (5), the circle integral is carried out along the perimeter of the billiard. The right-hand member of (5) defines an integral operator $\hat{Q}(k)$ acting on functions $\{u(s)\}$. Equation (5) admits non-trivial solutions $u(s)$ at the condition that the Fredholm determinant of the operator $\hat{I} - \hat{Q}(k)$ vanishes. Therefore, the real values of the wavenumber k where this condition is satisfied give the eigenvalues k^2 of the Helmholtz equation (1). The Fredholm determinant can be expanded in terms of its traces according to

$$0 = \det[\hat{I} - \hat{Q}(k)] = \exp - \sum_{N=1}^{\infty} \frac{1}{N} \mathrm{tr}\, \hat{Q}^N \tag{6}$$

with

$$\mathrm{tr}\, \hat{Q}^N = 2^N \oint \mathrm{d}s_1 \cdots \mathrm{d}s_N \frac{\partial G_0}{\partial n_1}(\boldsymbol{r}_1, \boldsymbol{r}_N) \frac{\partial G_0}{\partial n_N}(\boldsymbol{r}_N, \boldsymbol{r}_{N-1}) \cdots \frac{\partial G_0}{\partial n_3}(\boldsymbol{r}_3, \boldsymbol{r}_2) \frac{\partial G_0}{\partial n_2}(\boldsymbol{r}_2, \boldsymbol{r}_1) \tag{7}$$

where $\boldsymbol{r}_j = \boldsymbol{r}(s_j)$ belongs to the border of the billiard. Using the definition of the free Green function, we get

$$\frac{\partial G_0}{\partial n_{j+1}}(\boldsymbol{r}_{j+1}, \boldsymbol{r}_j) = -\frac{\mathrm{i}k}{4} \cos\varphi_{jj+1} H_1^{(1)}(k\ell_{jj+1}) \tag{8}$$

where φ_{jj+1} is the angle between the path from the point $\boldsymbol{r}_j$ to the point $\boldsymbol{r}_{j+1}$ and $\boldsymbol{n}_{j+1}$ is minus the unit vector normal to the border and interior to the billiard. $H_1^{(1)}(z)$ is the first Hankel function of first order and $\ell_{jj+1} = |\boldsymbol{r}_{j+1} - \boldsymbol{r}_j|$ is the length between those points. Introducing (8) in (7), we obtain

$$\mathrm{tr}\, \hat{Q}^N = \left(\frac{-\mathrm{i}k}{2}\right)^N \oint \mathrm{d}s_1 \cdots \mathrm{d}s_N \prod_{j=1}^{N} \left[\cos\varphi_{jj+1}\ H_1^{(1)}(k\ell_{jj+1})\right] \tag{9}$$

with the cyclic identification of the points $N+1$ and 1.

For numerical calculations, we used a discretized version of (5) to get the exact eigenvalues. In the following, we use (6)–(9) to calculate semiclassically the periodic orbit contributions to $N(k)$ which are given by

$$N(k)\Big|_{\mathrm{po}} = -\frac{1}{\pi} \lim_{\epsilon \to 0} \ \mathrm{Im} \log \det[\hat{I} - \hat{Q}(k + \mathrm{i}\epsilon)]\Big|_{\mathrm{po}} = \sum_{N=1}^{\infty} \frac{1}{\pi N} \mathrm{Im}\, \mathrm{tr}\, \hat{Q}(k)^N \Big|_{\mathrm{po}}. \tag{10}$$

3. Different contributions to $N(k)$

The geometry of the stadium is depicted in figure 1 together with examples of periodic orbits of α-, $\alpha\beta$-, and β-types. We denote by R the radius of the semicircles and by L the length of the straight walls. As a consequence, the periodic orbits of α- and $\alpha\beta$-types have lengths $4Rn$ which are multiples $n = 1, 2, \ldots$ of $4R$ because of the possibility of repeating the excursion over the fundamental period. In the following, we restrict ourselves to the periodic orbits of length $4R$ ($n = 1$). This simplification does not affect our conclusions. As we mentioned in the introduction, there is no β-orbit having a length with one of the values $4Rn$ so that the Gutzwiller contribution $N^{(\beta)}(k)$ do not contain any term corresponding to those lengths.

The periodic orbits of length $\ell = 4R$ make two bounces on the border of the billiard so that their contributions should appear in the term $N = 2$ of the series (10) which is given

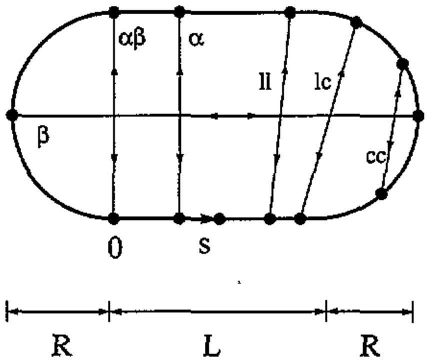

Figure 1. The different types of two-bounce periodic orbits of the stadium billiard. The isolated periodic orbits are labelled by β and the continuous family of bouncing-ball orbits by α. Finally, the $\alpha\beta$-orbits are the 'last' α-orbits which are bouncing at the matching points of the semicircles and straight walls. In the right-hand side, we show the three different paths—ll, lc, and cc—which contribute to the amplitude of the $\alpha\beta$-orbit. s is the coordinate of a point of the perimeter from the origin 0.

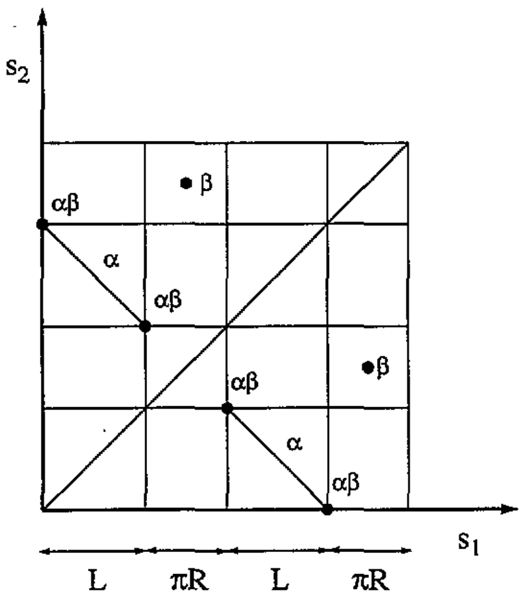

Figure 2. Domain of integration of equation (11) with the different critical points.

by (9). Using the property that $\ell_{12} = \ell_{21}$ and $\cos\varphi_{12} = \cos\varphi_{21}$ in the case where $N = 2$, the corresponding term becomes

$$\mathrm{tr}\hat{Q}^2 = \left(-\frac{ik}{2}\right)^2 \iint \mathrm{d}s_1 \mathrm{d}s_2 \left[\cos\varphi_{12} H_1^{(1)}(k\ell_{12})\right]^2 \tag{11}$$

where the double integral extends over the domain shown in figure 2.

In the semiclassical limit ($k \to \infty$), we can substitute the Hankel function by its asymptotic expansion [12]

$$H_1^{(1)}(z) \sim \sqrt{\frac{2}{\pi z}} \exp\left(\mathrm{i}z - \mathrm{i}\frac{3\pi}{4}\right) \qquad \text{for} \quad |z| \to \infty \tag{12}$$

so that (11) can be expressed as

$$\mathrm{tr}\hat{Q}^2 \sim -\frac{\mathrm{i}k}{2\pi} \iint \mathrm{d}s_1 \mathrm{d}s_2 \frac{\exp(2\mathrm{i}k\ell_{12})}{\ell_{12}}\,. \tag{13}$$

According to the stationary phase method, the main contributions to this integral are given by the critical points of the (s_1, s_2)-plane where the argument ℓ_{12} of the imaginary exponential is extremal. Those critical points are shown in figure 2. We find two segments of lines due to the bouncing ball α-orbits and two isolated points due to the unstable periodic β-orbits of Gutzwiller type. At the ends of the segments of lines, we find four points which are due to the edge $\alpha\beta$-orbits. We remark upon the twofold symmetry under the exchange of the integration variables $s_1 \leftrightarrow s_2$.

An essential aspect is that the stadium is composed of four geometric elements which have different curvatures: the two straight walls and the two semicircles. As a consequence, the double integral (13) decomposes into 16 different integrals. Around the α and the $\alpha\beta$ critical points, we find integrals of three kinds depending on whether the two bounces occur between the two straight walls (ll), between a straight wall and a semicircle (lc), or between two points of the same semicircle (cc) as shown in figure 1. (In these notations, l stands for line and c for circle.) In all those cases, we may expand the length of the path into a Taylor series in terms of local variables $x_1 = s_1 - s_1^0$ and $x_2 = s_2^0 - s_2$ which vanish at the critical point

$$\ell_{12} = \ell(s_1, s_2) = 2R + \frac{1}{4R}\boldsymbol{x}^{\mathrm{T}} \cdot \mathbf{A} \cdot \boldsymbol{x} + O(x^4)\,. \tag{14}$$

$\mathbf{A}$ is a 2×2-matrix which may be degenerate or not. (The matrix is degenerate if at least one eigenvalue is zero.) We remark that the previous division of the integration domain corresponds to the discontinuities in the second derivatives of the length (14) so that different matrices $\mathbf{A}$ are defined in the three cases: ll, lc, cc. Let us evaluate their contributions separately.

3.1. The line–line integral

In this case, the critical point corresponds, for instance, to the line $s_1 = 2L + \pi R - s_2$. We introduce the local coordinates, $x_1 = s_1$ and $x_2 = 2L + \pi R - s_2$. The critical points are now $0 < x_1 = x_2 < L$ and the matrix $\mathbf{A}$ is

$$\mathbf{A}_{\mathrm{ll}} = \begin{pmatrix} 1 & -1 \\ -1 & 1 \end{pmatrix} \tag{15}$$

which is degenerate with eigenvalues $2, 0$. The ll contribution to (13) is, therefore,

$$\mathrm{tr}\hat{Q}^2\Big|_{\mathrm{ll}} \sim -\frac{\mathrm{i}k}{2\pi R} \exp(\mathrm{i}4kR) \int_S \mathrm{d}x_1 \mathrm{d}x_2 \exp\left[\frac{\mathrm{i}k}{2R}(x_1 - x_2)^2\right] \tag{16}$$

where a factor of two has been included to take the twofold symmetry $s_1 \leftrightarrow s_2$ into account and where the domain of integration is $S = \{0 < x_1 < L; 0 < x_2 < L\}$. We make a change of integration variables toward $x = (x_1+x_2)/2$ and $y = x_1 - x_2$ with $dx_1\,dx_2 = dx\,dy$. The integral over the square S is decomposed according to

$$\iint_S = \iint_\Omega - 4\iint_\omega \tag{17}$$

into an integral over the rectangle $\Omega = \{0 < x < L; -L < y < +L\}$ minus four integrals to remove the contributions from the corners $\omega = \{0 < x < y/2; 0 < y < L\}$.

The integration in the domain Ω gives the Berry–Tabor term for two bounces ($N = 2$). We can show that the Berry–Tabor formula is obtained by extending the previous integration to the other terms of (9) corresponding to the multiple repetitions of the α-orbit as will be reported elsewhere [13]. On the other hand, the integrals over the domain ω concern the edge orbits of $\alpha\beta$-type.

Finally, we get

$$\mathrm{tr}\,\hat{Q}^2\Big|_{\mathrm{ll}} \sim L\sqrt{\frac{k}{2\pi R}}\exp\left(\mathrm{i}4kR - \mathrm{i}\frac{\pi}{4}\right) - \frac{1}{\pi}\exp(\mathrm{i}4kR)\,. \tag{18}$$

We remark that the first term is of order $\sqrt{k}$ while the second one is in k^0 like the Gutzwiller contributions.

3.2. *The line–circle and circle–circle integrals*

Let us introduce the local coordinates $x_1 = s_1 - L$ and $x_2 = L + \pi R - s_2$ so that the second derivative matrices are

$$\mathbf{A}_{\mathrm{lc}} = \begin{pmatrix} 1 & -1 \\ -1 & -1 \end{pmatrix} \qquad \mathbf{A}_{\mathrm{cc}} = \begin{pmatrix} -1 & -1 \\ -1 & -1 \end{pmatrix}. \tag{19}$$

In both cases, the critical points are isolated points appearing at a corner of the integration domain (see figure 2). The corner forms an angle of 90 degrees so that it is natural to introduce the polar coordinates $\boldsymbol{x} = (x_1, x_2) = (2R\rho/k)^{1/2}\boldsymbol{u}$ with the unit vector $\boldsymbol{u} = [\cos(\theta+\alpha), \sin(\theta+\alpha)]$ where $\alpha_{\mathrm{lc}} = \pi/2$ and $\alpha_{\mathrm{cc}} = 0$. In terms of the new variables (ρ, θ) the integrals become

$$\mathrm{tr}\,\hat{Q}^2\Big|_{\mathrm{lc,cc}} \sim \lim_{\epsilon\to 0} -\mathcal{N}_{\mathrm{lc,cc}}\frac{\mathrm{i}}{4\pi}\exp(\mathrm{i}4kR)\int_0^{\pi/2}\mathrm{d}\theta\int_0^{\infty}\mathrm{d}\rho\,\exp\left(\mathrm{i}\rho\boldsymbol{u}^{\mathrm{T}}\cdot\mathbf{A}\cdot\boldsymbol{u} - \epsilon\rho\right) \tag{20}$$

where ϵ is introduced to allow us to take the limit $\rho \to \infty$ in the integral. The integer factor counts the number of times the corresponding corner contributes: $\mathcal{N}_{\mathrm{lc}} = 8$ and $\mathcal{N}_{\mathrm{cc}} = 4$.

If we evaluate the integral over the radial variable in (20), we obtain the well known distribution

$$\frac{1}{z + \mathrm{i}\epsilon} = \mathcal{P}\frac{1}{z} - \mathrm{i}\pi\delta(z) \tag{21}$$

where $\mathcal{P}$ is the Cauchy principal value of the integral and $\delta(z)$ is the Dirac distribution. As a consequence, we get

$$\mathrm{tr}\,\hat{Q}^2\Big|_{\mathrm{lc,cc}} \sim \mathcal{N}_{\mathrm{lc,cc}}\frac{\mathrm{e}^{\mathrm{i}4kR}}{4\pi}\left[\mathcal{P}\int_0^{\pi/2}\frac{\mathrm{d}\theta}{\boldsymbol{u}^{\mathrm{T}}\cdot\mathbf{A}\cdot\boldsymbol{u}} - \mathrm{i}\pi\int_0^{\pi/2}\mathrm{d}\theta\,\delta(\boldsymbol{u}^{\mathrm{T}}\cdot\mathbf{A}\cdot\boldsymbol{u})\right]. \tag{22}$$

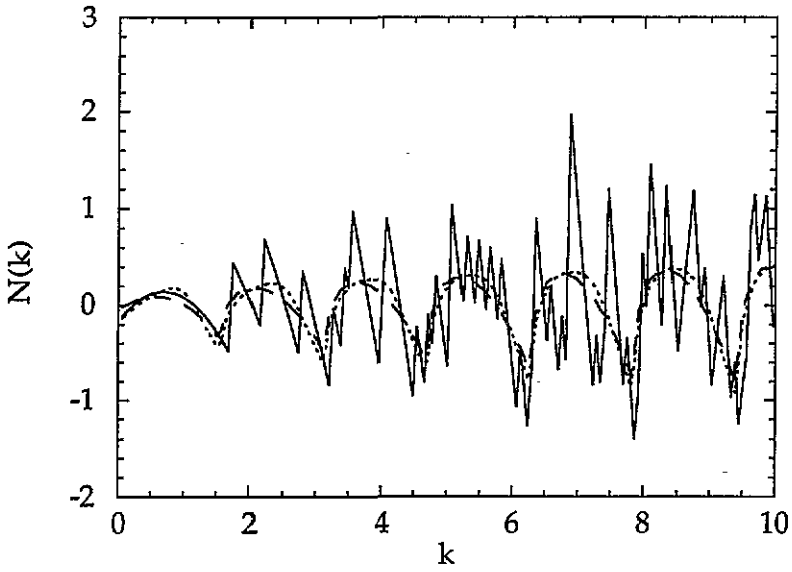

Figure 3. Oscillatory behaviour of the staircase function $N(k)$. The full line represents the exact quantum mechanical result for $N_{\mathrm{exact}}(k) - N_{\mathrm{av}}(k)$ obtained numerically. ($N_{\mathrm{av}}(k)$ is the non-oscillatory part containing the area, perimeter and curvature terms.) The dashed line is the prediction of the Berry–Tabor formula (28) while the dotted line is given by the Berry–Tabor formula plus the first term (26) of the contribution of the $\alpha\beta$-orbits. The remaining oscillations present in the full line correspond to the Gutzwiller term.

The second term contributes only if $\boldsymbol{u}^{\mathrm{T}} \cdot \mathbf{A} \cdot \boldsymbol{u}$ vanishes in the interval $0 < \theta < \pi/2$, which happens in the line–circle but not in the circle–circle case.

Performing the integrals, we finally get

$$\mathrm{tr}\hat{Q}^2\Big|_{\mathrm{lc}} \sim \frac{\sqrt{2}}{\pi}\left[\ln(1+\sqrt{2}) - \mathrm{i}\frac{\pi}{2}\right]\exp(\mathrm{i}4kR) \tag{23}$$

$$\mathrm{tr}\hat{Q}^2\Big|_{\mathrm{cc}} \sim -\frac{1}{\pi}\exp(\mathrm{i}4kR)\,. \tag{24}$$

Summing the contributions (18), (23), and (24) and using the term $N = 2$ of (10), we finally obtain that the two-bounce periodic orbits of length $\ell = 4R$ contribute to the staircase function by the term $N_2^{(\alpha)}(k) + N_2^{(\alpha\beta)}(k)$, where

$$N_2^{(\alpha)}(k) \sim \frac{L}{2\pi}\sqrt{\frac{k}{2\pi R}}\,\cos\left(4kR - \frac{3\pi}{4}\right) \tag{25}$$

$$N_2^{(\alpha\beta)}(k) \sim \frac{A}{2\pi}\sin(4kR + B) \tag{26}$$

$$\text{with}\quad A = 0.746\,68 \quad\text{and}\quad B = 1.243\,76 + \pi\,. \tag{27}$$

The first term is part of the Berry–Tabor formula while the second term is the new contribution from the edge orbits.

4. Numerical comparison

In order to establish a comparison, we have numerically calculated the spectrum of the stadium with $R = 1$ and $L = 2.4$ in the interval of wavenumbers $k_{\min} = 0 < k < k_{\max} = 9.99$ containing the first 55 eigenvalues. In figure 3, we have plotted the oscillatory part $N_{\rm exact}(k) - N_{\rm av}(k)$ of the staircase function. The exact function is compared with the full Berry–Tabor contribution from the bouncing-ball orbit

$$N^{(\alpha)}(k) = \frac{L}{2\pi}\sqrt{\frac{k}{2\pi R}}\sum_{n=1}^{\infty} n^{-3/2}\cos\left(4knR - \frac{3\pi}{4}\right) \tag{28}$$

as well as with $N^{(\alpha)}(k) + N_2^{(\alpha\beta)}$ which fits better with the exact function.

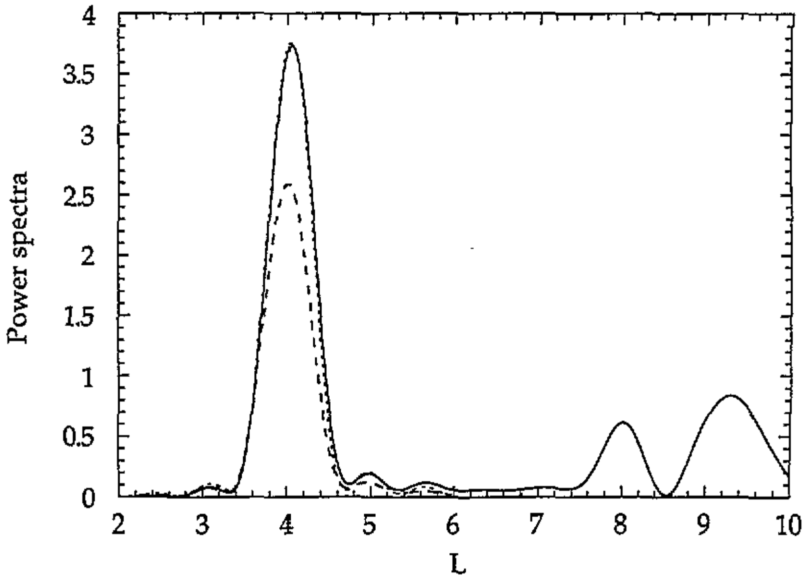

Figure 4. Power spectra of the functions of figure 3 calculated with (4) with $k_{\min} = 0$ and $k_{\max} = 9.99$. The peaks at $\ell = 4$ and 8 correspond to the shortest α- and $\alpha\beta$-orbits while the other peak is related to the group of isolated orbits of lengths around $\ell = 9.5$ starting at $\ell = 8.8$ (shortest β-orbit). Like in figure 3, the dashed line is the prediction of the Berry–Tabor formula (28) while the dotted line gives the amplitude obtained when the $\alpha\beta$-term (26) is moreover added to (28).

Figure 4 shows the length spectrum defined by (4) around the length $\ell = 4R$. The length spectrum $S_{\rm exact}(\ell)$ calculated with the exact staircase function is compared with the functions $S^{(\alpha)}(\ell)$ calculated by including only the Berry–Tabor contribution from the α-orbits. We see that the Berry–Tabor term only contributes to 60% of the peak at the length $\ell = 4R$. This discrepancy is removed if we add the contribution from the edge orbits as seen with the third function $S^{(\alpha)+(\alpha\beta)}(\ell)$ in figure 4. The agreement is then excellent and sustains the statement that the edge orbits have a considerable contribution to the staircase function of the stadium which cannot be explained by either the Berry–Tabor or the Gutzwiller formula. We remark that the edge orbits are also contributing to the length spectrum at the multiples $\ell = 4nR$ of the length of the bouncing-ball orbit.

5. Conclusions

In conclusion, we have shown in this paper that the contribution of edge orbits plays an important role in the staircase function of the stadium which should be given by

$$N_{\text{exact}}(k) \sim N_{\text{av}}(k) + N^{(\alpha)}(k) + N^{(\alpha\beta)}(k) + N^{(\beta)}(k) \qquad \text{for} \quad k \to \infty \tag{29}$$

with the new term (26) correcting (3). The order of magnitude of the contribution of the edge orbits appears to be of the same order as that of the Gutzwiller term and so to come after the Berry–Tabor term in the semiclassical expansion of the staircase function. How the edge orbits contribute to the semiclassical quantization is an open question because we also need the contributions of the repetitions of the edge orbits for that purpose.

At the end of the present work, a recent preprint by Sieber *et al* came to our knowledge where the contribution of the edge orbits has been derived for the desymmetrized stadium billiard. In the case of the desymmetrized billiard, it turns out that the contribution of the edge orbits is much smaller than for the full billiard.

Clearly, the nature of the new contributions we have described in this paper lies with the fact that the curvature of the boundary of the billiard is discontinous. Accordingly, we believe that these diffraction effects will also appear in other billiards sharing this feature with the stadium.

Acknowledgments

It is our pleasure to thank Professor G Nicolis for support and encouragement. We thank Professor J W Turner for fruitful discussions and Y Shimizu for pointing out mistakes in the original manuscript. DA is grateful to A Padilla and J Perez for encouragement. DA is financially supported by the CEE Human Capital and Mobility Project under contract no ERBCHBICT920097 and PG by the National Fund for Scientific Research (FNRS Belgium). This research was supported by the CEE Science Project SADOVEM under contract no SC1-CT91-0711.

References

[1] Gaspard P and Rice S A 1989 *J. Chem. Phys.* **90** 2225, 2242, 2255; 1993 *Phys. Rev.* A **48** 54
[2] Cvitanović P and Eckhardt B 1989 *Phys. Rev. Lett.* **63** 823–6
[3] Ezra G S, Richter K, Tanner G and Wintgen D 1990 *J. Phys. B: At. Mol. Phys.* **4** L413–L420
[4] Sieber M 1991 The hyperbola billiard: A model for the semiclassical quantization of chaotic systems *PhD Thesis*
[5] Bunimovich L A and Sinai Ya G 1980 *Commun. Math. Phys.* **78** 247, 479
[6] Graf H D, Harney H L, Lengeler H, Lewenkopf C H, Rangacharyulu C, Richter A, Schardt P and Weidenmüller H A 1992 *Phys. Rev. Lett.* **69** 1296
[7] Balian R and Bloch C 1970 *Ann. Phys.* **60** 401–47
Balian R and Bloch C 1972 *Ann. Phys.* **69** 76–160
[8] Gutzwiller M C 1971 *J. Math. Phys.* **12** 343–58
[9] Berry M V and Tabor M 1976 *Proc. R. Soc.* A **349** 101–23
Berry M V and Tabor M 1977 *J. Phys. A: Math. Gen.* **10** 371
[10] Berry M V 1984 *Proc. R. Soc.* A **392** 15–43
[11] Gaspard P 1993 *Quantum Chaos* ed G Casati, I Guarneri and U Smilansky *Proc. Int. School of Physics Enrico Fermi (Varenna)* (Amsterdam: North-Holland) 307–83
[12] Abramowitz M and Stegun I A 1972 *Handbook of Mathematical Functions* (New York: Dover)
[13] Alonso D and Gaspard P, in preparation
[14] Sieber M, Smilansky U, Creagh S C and Littlejohn R G 1993 Non-generic spectral statistics in the quantized stadium billiard *WIS-preprint*